Summer November 19, 2014

Implementation of a modified perturb and observe maximum power point tracking algorithm for photovoltaic system using an embedded microcontroller

Dr. Adel A. Elbaset

IET Renewable Power Generation

Research Article

Implementation of a modified perturb and observe maximum power point tracking algorithm for photovoltaic system using an embedded microcontroller

ISSN 1752-1416
Received on 10th July 2015
Revised on 8th September 2015
Accepted on 30th September 2015
doi: 10.1049/iet-rpg.2015.0309
www.ietdl.org

Adel A. Elbaset[1,2], Hamdi Ali[3], Montaser Abd-El Sattar[3] ✉, Mahmoud Khaled[4]

[1]*Department of Electrical Engineering, Minia University, Minia 61517, Egypt*
[2]*Faculty of Postgraduate Studies for Advanced Science, Beni-Suef University, Beni-Suef, Egypt*
[3]*Department of Electrical and Computer Engineering, El-Minia High Institute for Engineering and Technology, Minia, Egypt*
[4]*Department of Computer and Systems Engineering, Minia University, Minia 61517, Egypt*
✉ *E-mail: adel.soliman@mu.edu.eq*

Abstract: The conventional algorithm of perturb and observe (P&O) is widely applied due to its simplicity, low cost and easy implementation. However, it suffers from instabilities during rapid changes of weather and/or oscillation around maximum power point (MPP) at steady state. Instabilities occur due to the incorrect decision taken by the conventional P&O algorithm at the first step change in duty cycle during the rapid change in radiation. The reason for the steady-state oscillation is the continuous perturbation and tradeoff between step sizes and the convergence time. This study presents a modified P&O algorithm to overcome such drawbacks. It uses a constant load technique to help the conventional P&O algorithm for recognising the cause of power change and to enable it in taking the right decision at first step change in duty cycle during rapid change of weather. The proposed algorithm is simulated using a single solar photovoltaic module of 80 W and a DC/DC boost converter. It is validated experimentally and implemented within an embedded microcontroller. The experimental setup presents a proposed model-based design methodology that uses measurements' data for MPP tracking systems' design. It combines hardware-in-the-loop simulation and prototype testing using actual weather measurements. Simulation and experiments show excellent results.

1 Introduction

The increasing growth of photovoltaic (PV) system is expected to reach 800 GW by the year 2030. This growth of PV systems market is because they are available, requires free energy source (the sun), abundant, maintainable and pollution free [1–4]. Although PV systems have many benefits, they face three major problems. One of them is their low efficiency that can hardly reach 20%, while the two others are the change of the produced electric power with respect to weather variations and non-linearity of their electrical characteristics [2, 5–7]. Normally, the efficiency of PV system mainly depends on solar irradiance level and atmospheric temperature [8]. Therefore, PV systems should be operated at maximum power point (MPP) to achieve the highest possible efficiency [7–11]. An MPP tracking (MPPT) system is one of the vital components that every PV system should include to ensure that the highest possible power is generated. It is an electronic control system, which monitors PV terminal voltage/current and achieve MPP by controlling the duty cycle of a DC/DC converter to match output load to PV source impedance [7–11]. Efficient MPPT systems should track MPP at all times whatever the weather conditions or load are being. They should be simple, accurate and economically implementable [6, 11, 12].

Numerous MPPT algorithms are available in industry and academia, which have many particular/general applications [7–11]. Each algorithm has specialised technique according to its control variables like voltage, current and its duty cycle [2, 11]. The most famous MPPT algorithms are based on: perturb and observe (P&O) [2, 7, 8, 13], incremental conductance [5, 14, 15], hill climbing [16–18], direct control [5], fuzzy logic control [19, 20], artificial neural networks [21, 22], genetic algorithms [23], particle swarm optimisation [24, 25], short-current pulse [6], constant voltage [6] and sliding mode control [26]. These algorithms are differing from each other in terms of number of sensors used, complexity in algorithm and implementation cost [6]. Their main objective is to achieve fast and accurate tracking performance and to minimise oscillations due to varying weather conditions [2].

Among all the mentioned algorithms, the P&O algorithm is the most popular and widely used due to its simplicity, ease of implementation and low cost [2, 7, 8, 13]. However, the algorithm fails when tracking MPP during rapid change of weather. In addition, its tracking performance has steady-state oscillations around MPP according to step size [8, 10, 24].

The main contributions of this paper are:

- Explanation of conventional P&O algorithm performance during weather and load change as shown in Section 2.
- The presentation of modified P&O (MP&O) algorithm to overcome previous drawbacks of conventional P&O algorithm. This is presented in Section 3.
- The presentation of PV system simulation based on two-diode model [27, 28]. This is presented in Section 4.
- The presentation of a model-based design methodology that combines hardware-in-the-loop (HIL) simulation, prototype testing and actual weather measurements. This methodology offers more successful and rapid design flow. This is presented in Section 5.
- An example tutorial-like case study for the implementation of the proposed algorithm within an embedded real-time microcontroller system using the proposed design methodology. This is also presented in Section 5.

2 Concept of conventional P&O algorithm

Conventional P&O algorithm is the simplest, cheapest and most popularly used in practice [16]. However, it is not robust in tracking the right MPP at rapid changes of weather or load [7, 13, 24, 29]. The flowchart of the basic P&O MPPT algorithm is presented in Fig. 1*a*. The basic P&O scans the $P-V$ curve of PV module in search for the MPP by changing the operating point which is known as perturbation step, and then measuring the change in P (ΔP), known as observation step. If ΔP is greater than zero, then a new perturbation is introduced in the same direction. If ΔP is lower than zero, the direction of the perturbation is changed. The P&O keeps searching for the MPP until it has found an operating point such that ΔP is closely to zero in any direction; this condition is called steady state. At steady state, the operating point oscillates around the MPP giving rise to the wastage of some amount of

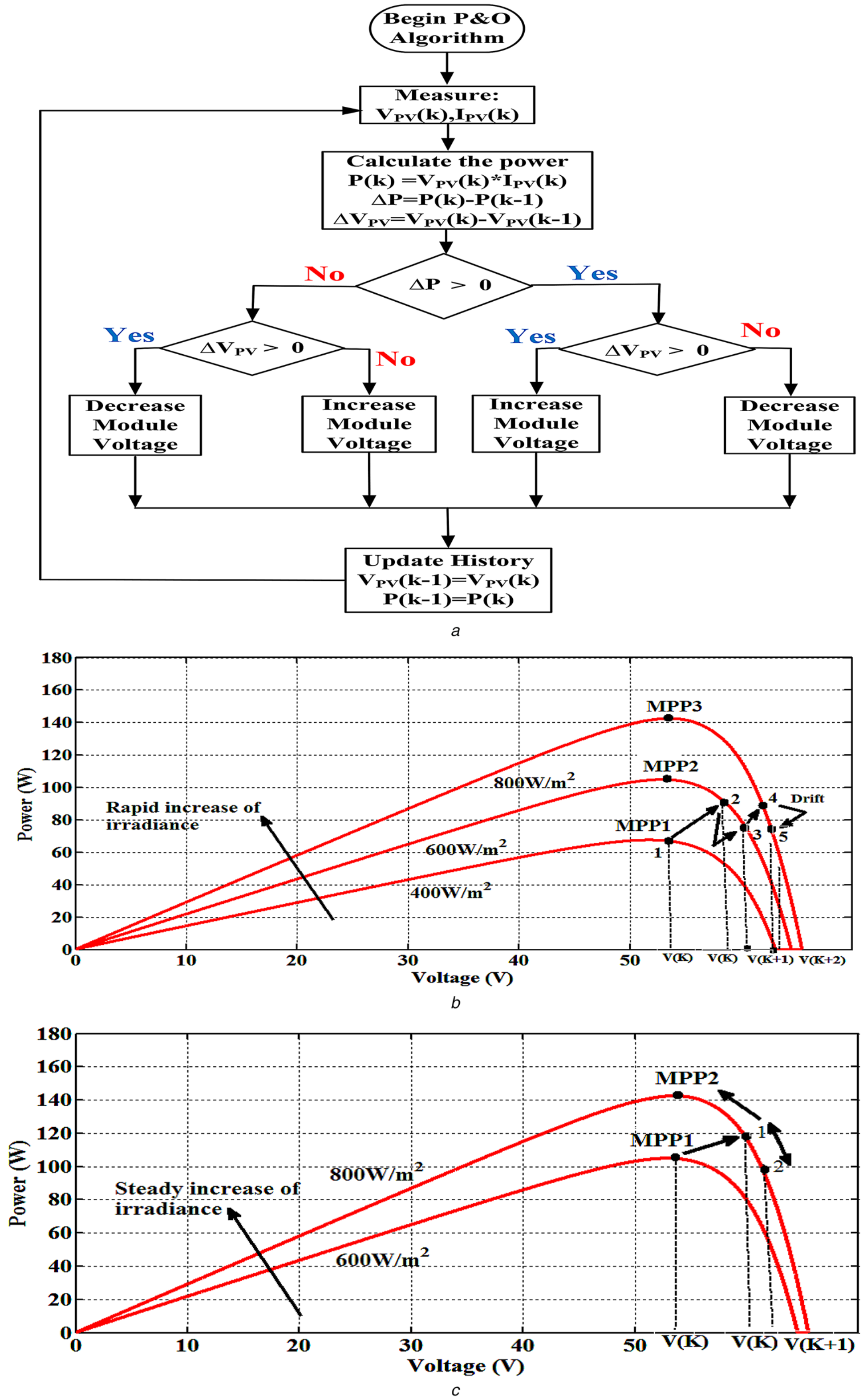

Fig. 1 *Conventional P&O algorithm and radiation change*

a Flowchart of conventional P&O algorithm [29]
b Simulation results of rapid increasing in radiation
c Simulation results of steady change in radiation

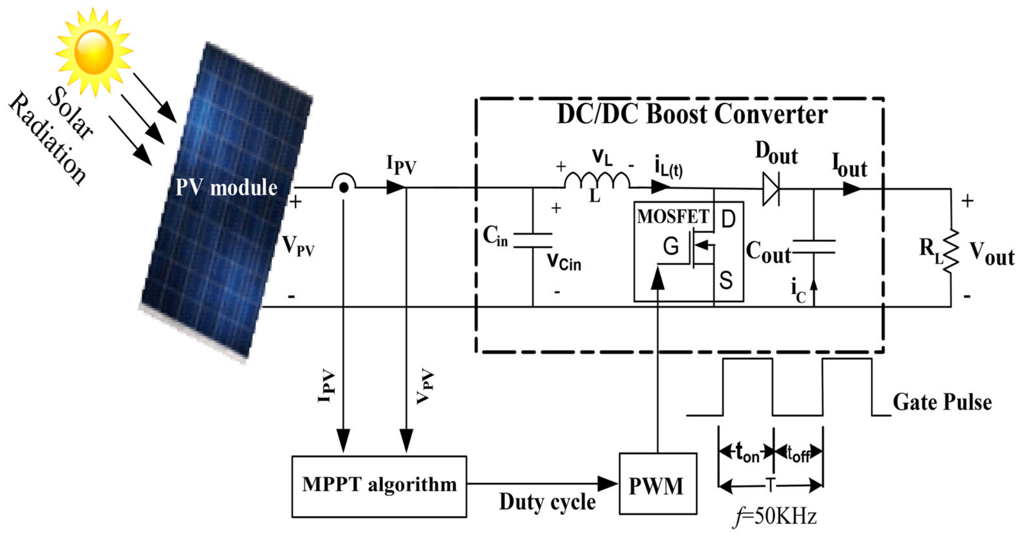

a

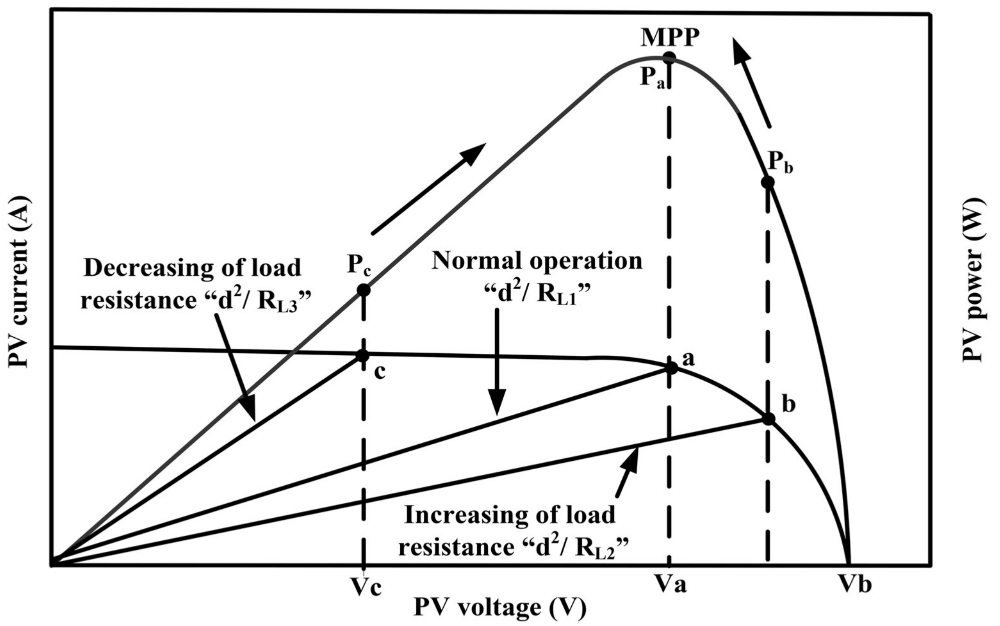

b

Fig. 2 *MPPT system and load change*

a Schematic diagram of MPPT system
b Change of operating point with respect to load resistance

available energy. These oscillations can be minimised by reducing the fixed step size, but it takes relatively more time to reach MPP. The P&O keeps perturbing the system in order to detect a change in the MPP (caused by a change in the environmental conditions), which triggers a new scan [7, 8].

2.1 Performance of conventional P&O algorithm during rapid change of radiation

The successive rapid increasing of radiation causes drift or instability problem due to conventional P&O algorithm. Suppose there is an increase in radiation level from 600 to 1000 W/m^2 and the PV system operates at point MPP1 at perturbation K as shown in Fig. 1*b*. Then, the operating point will be moved to a new point 2 in corresponding radiation curve during the same perturbation K which results in positive change in both power (ΔP) and voltage (ΔV) [13, 30–33]. The information of positive change in power and voltage during perturbation $K+1$ will make algorithm to increase voltage perturbation instead of decreasing. Hence, the operating point moves from point 2 to point 3 as shown in Fig. 1*b*. This wrong decision of conventional P&O algorithm causing the operating point of PV system is deviated away from MPP as a result of successive change of weather as shown in Fig. 1*b*. Moreover, the successive rapid decreasing of radiation will deviate the operating point of PV system away from MPP as discussed in [2].

2.2 Behaviour of conventional P&O algorithm during steady change of radiation

The steady change of weather will cause wrong decision of P&O algorithm at first perturbation as discussed in rapid change of weather, but the next perturbation will correct this wrong action [8]. Suppose there is an increase in radiation level from 400 to 600 W/m^2 and the PV system operates at MPP1 as shown in Fig. 1*c*. Then increasing of PV power and voltage will increase voltage perturbation and the operating point from MPP2 will divert at point 2 as shown in Fig. 1*c*. The next perturbation on the same *P*–*V*

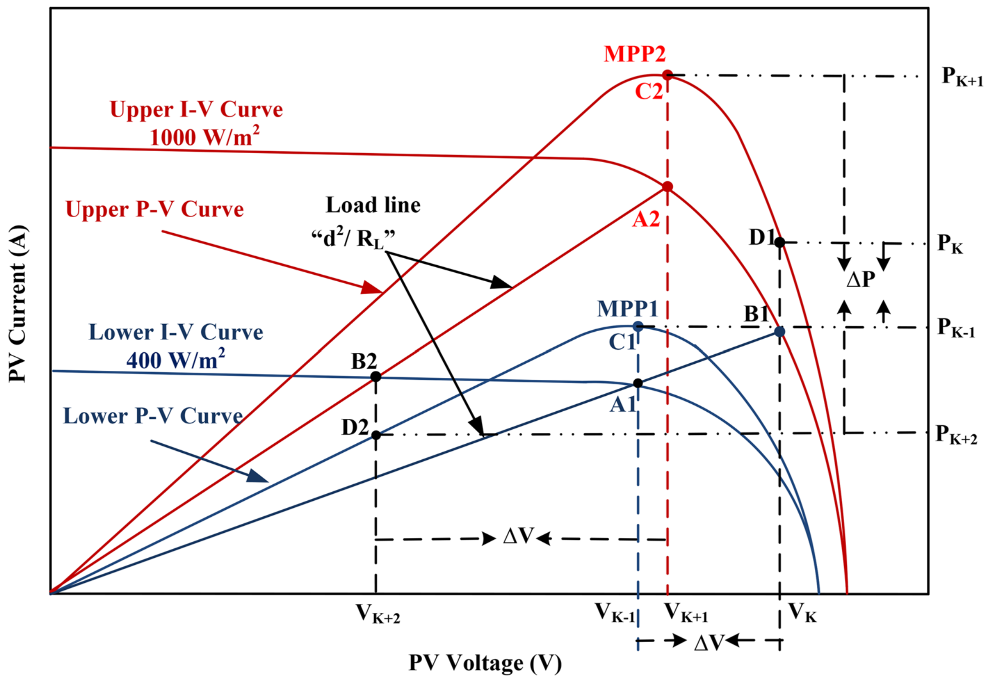

Fig. 3 *PV power and voltage due to weather variations*

curve – without weather change – will be negative change in PV power ($\Delta P < 0$) and the positive change in PV voltage ($\Delta V > 0$) causing decrease in the voltage perturbation towards MPP2 with subsequent next perturbations as shown in Fig. 1*c*.

2.3 Conventional P&O algorithm and load change

The PV load (R_L) is connected across PV terminal via DC/DC boost converter as shown in Fig. 2*a*. The DC/DC boost converter matched the load impedance with source impedance of the PV system to satisfy maximum power transfer. In addition, P&O MPP trackers enable PV systems to operate at MPP.

The relations between input and output variables of DC/DC boost converter are expressed as follows [8, 13, 34, 35]

$$V_{\text{out}} = d * V_{\text{PV}} \tag{1}$$

$$I_{\text{out}} = I_{\text{PV}}/d \tag{2}$$

$$d = 1/(1 - D) \tag{3}$$

$$S_L = I_{\text{PV}}/V_{\text{PV}} = d^2(I_{\text{out}}/V_{\text{out}}) = d^2/R_L \tag{4}$$

$$R_L = d^2(V_{\text{PV}}/I_{\text{PV}}) \tag{5}$$

where V_{out} and I_{out} are output voltage and current of boost converter, d is a linear control variable between V_{out} and V_{PV}, D is the duty cycle, S_L is the slope of load line and R_L is the output load resistance of DC/DC boost converter.

The operating point of the PV system is determined by the slope of load line as shown in Fig. 2*b*. This slope will change the operating point on *I–V* characteristic curve of the PV system by changing the linear variable '*d*' or load resistance. The algorithm will take this variable as controlled variable for voltage change and then computes the duty cycle from (3) as follows

$$D = (d - 1)/d \tag{6}$$

Normally, the PV system operates close to MPP at steady weather and without change in load as shown in Fig. 2*b*. The load change causes the operating point of the PV system to move away – either right or left side – from MPP at point a of Fig. 2*b*. The increasing in load resistance from R_{L1} to R_{L2} will move the operating point to the right side of MPP at point b that is causing decrease in power and increase in voltage. The negative change in PV power ($\Delta P < 0$) and positive change in PV voltage ($\Delta V > 0$) will decrease the perturbation voltage as illustrated from flowchart of Fig. 1*a* [29]. The positive change in power and negative change in voltage in subsequent perturbation will decrease the voltage at the same direction to MPP. Moreover, the decreasing of load resistance from R_{L1} to R_{L3} will move the operating point to the left side of MPP at point c of Fig. 2*b*. This action will cause negative change in both power and voltage that are causing the algorithm to increase the PV voltage towards MPP [8].

2.4 Description of conventional P&O algorithm problem

As mentioned before, the conventional P&O algorithm has poor tracking of MPP for weather change and good tracking for load change at constant weather. This poor tracking of MPP is due to the algorithm cannot distinguish the cause of power change either is coming from weather variation or perturbation step due to load change. The MPPT moves away from the real MPP due to the quick change in the weather condition. In addition, steady-state oscillations are due to tradeoffs between step size and tracking speed of MPP.

3 MP&O algorithm

3.1 Basic modification

The performance of conventional P&O algorithm as previously stated can be divided into weather change under constant load and load change under constant weather. The conventional P&O algorithm has its best performance with load change under constant weather, but it has a poor performance with weather change under fixed load. To enhance the performance of conventional P&O algorithm due to weather change under constant load (R_L), it should be modified to recognise this condition during rapid change or steady change of radiation by computing a load value (R_L) in every perturbation step to ensure unchangeable of load and the change in power is coming from weather change. Additionally, the load change (ΔR_L) is apparent under constant weather conditions and therefore the algorithm recognises that power change is due to load change.

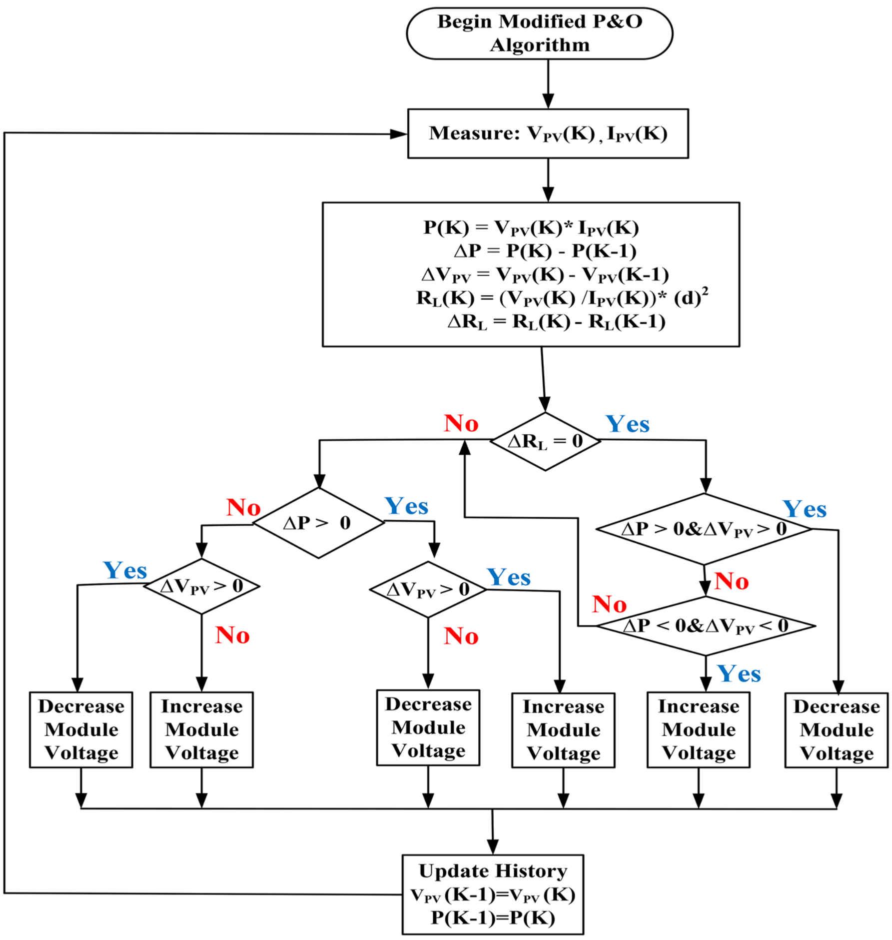

a

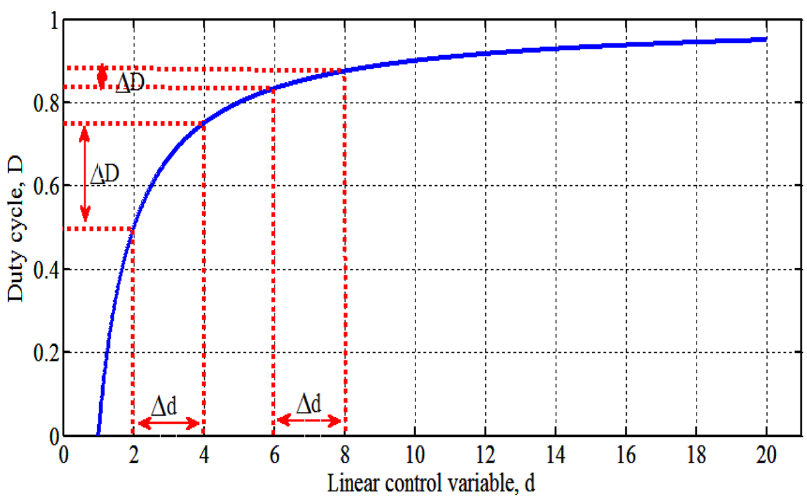

b

Fig. 4 *MP&O algorithm and radiation change*

a Flowchart of MP&O algorithm
b Relationship between '*D*' and variable '*d*'

3.2 Modification procedures due to weather change

It is observed that the conventional P&O algorithm is only based on a single *P–V* or *I–V* characteristic curve, and all perturbations are focused on it. These perturbations have not taken into account variations of weather. Normally, weather variations occur at least between two *P–V* characteristic curves [7, 13, 17]. Consequently, the conventional P&O algorithm should then recognise the variation of the PV power between these *P–V* curves under constant load. The following steps explain the MP&O algorithm:

I. During perturbation *K* suppose that, the solar radiation is increased from 400 to 1000 W/m^2 under constant load 'R_L'. The increasing of weather will move the operating point of PV system from point 'A1' on low radiation *I–V* curve to point 'B1' on upper high

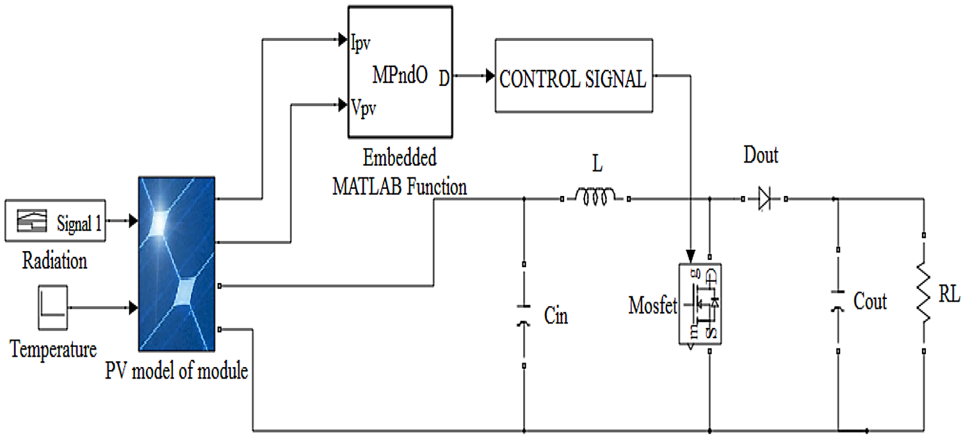

Fig. 5 *PV system model on Matlab/Simulink*

radiation *I–V* curve as shown in Fig. 3. The transferring of the operating point will increase the PV voltage from point 'A1' on low radiation *I–V* curve to point 'B1' on upper high radiation *I–V* curve. Moreover, the PV power point 'C1' that is located on MPP1 of low radiation *P–V* curve will change to point 'D1' that is far away from MPP2 on the upper high radiation *P–V* curve.

II. Both increasing of PV power and voltage under constant load from low to upper high radiation *I–V* and *P–V* curves of Fig. 3, will give positive change in power $\Delta P > 0$, $\Delta P = P(k) - P(k-1)$ and positive change in voltage $\Delta V > 0$, $\Delta V = V(k) - V(k-1)$ without change in load resistance. Both positive change in power ($\Delta P > 0$) and voltage ($\Delta V > 0$) under constant load ($\Delta R_L = 0$) will orient algorithm to decrement voltage perturbation to obtain MPP2 of Fig. 3. MPP is the main goal of algorithm to optimise the PV power.

III. Suppose that the solar radiation is decreased from 1000 to 400 W/m^2 during perturbation $K+1$ of P&O algorithm. The reducing of radiation level will reduce voltage level and move the operating point from point 'A2' on upper high radiation *I–V* curve to point 'B2' on low radiation *I–V* curve as shown in Fig. 3. The transferring of operating point will also decrease the PV power from point 'C2' that is located on MPP2 on upper high radiation *P–V* curve to point 'D2' that is deviated from MPP1 on low radiation *P–V* curve as illustrated in Fig. 3 under fixed load with negative change in power $\Delta P < 0$, $\Delta P = P(k+2) - P(k+1)$ and negative change in voltage $\Delta V < 0$, $\Delta V = V(k+2) - V(k+1)$. Both negative change in power and voltage under constant load ($\Delta R_L = 0$) will orient algorithm to increment voltage perturbation to reach MPP1 of Fig. 3. Optimising of power is satisfied for algorithm by extracting MPP.

IV. When the load is varied under constant weather condition, the conventional P&O algorithm will track MPP of PV system with best performance.

According to the described modifications to the conventional P&O algorithm, the load resistance (R_L) will help recognising the cause of power variation which is either coming from weather or load. The combination of both weather and load change techniques will result in a MP&O algorithm. This algorithm can distinguish whether the change in power is coming from weather or load as shown in its flowchart of Fig. 4*a*.

3.3 Fast tracking of MPP with reducing oscillations

The steady-state oscillations of conventional P&O algorithm are minimised with fast tracking of MPP using a variable '*d*' that gives linear relation between input and output voltages [34, 35]. This variable has an efficient effect on the duty cycle '*D*' to speed up the algorithm to track MPP. The relation between duty cycle and that variable is given from (6). It can be seen from (6) and Fig. 4*b* that, the duty cycle and its step size (ΔD) have variable values with variable *d* and its regular step change. Fig. 4*b* indicates a large variation of the duty cycle at lower values of '*d*' and smaller variation of *D* at higher values of *d* which satisfied the optimum requirements at $d \geq 1$ of extracting MPP. The reduce change of *D* at high values of *d* will reduce the oscillations at steady state. Normally, the zero value is floating point due to truncation error and cannot be determined with the precious practical manner which is close to it [15, 33]. Hence, it should assume a precious value that is below it, and the algorithm will fix the duty cycle to minimise steady oscillations to zero without considering the loss of PV power. To satisfy this requirement, the minimum change in power with respect to its power ($\Delta P/P$) is proposed less than the precious value 'ε'. If the change in power ($\Delta P/P$) is proposed less than $\varepsilon \leq 0.006$, the algorithm will fix the value of '*d*' and consequently the duty cycle.

4 Simulation results of large step irradiance

Fig. 5 presents simulation components for the modified algorithm: a single 80 W PV module modelled using the two-diode technique, the MP&O algorithm, a DC/DC boost converter and a load (R_L). The parameters of the PV model and the DC/DC converter are given in Table 1. The parameters of the two-diode model are computed from the datasheet parameters using Newton–Raphson method [27, 28].

Fig. 6 depicts simulation results of both conventional and modified algorithms under same conditions during rapid changes of radiation. At $G = 0.4$ kW/m^2, the maximum extractable power (shown in green dashed line) is 29.5 W. At $t = 2$ s, radiation is suddenly changed from 0.4 to 1.0 kW/m^2, causing an increase in the maximum extractable power to reach 80 W. At $t = 6$ s, radiation is stepped down to $G = 0.4$ kW/m^2. Temperature is kept constant at 25°C for all radiation levels. It is observed that the performance of the proposed algorithm is better than the conventional one. It is capable of minimising steady-state oscillations at either increasing or decreasing radiation. During quickly varying weather conditions, the conventional P&O

Table 1 Parameters of 80 W module and DC/DC boost converter

80 W module [28]		Two-diode model		DC/DC boost converter	
Parameter	Value	Parameter	Value	Parameter	Value
P_{mp}, W	80.0	I_{ph}, A	5.1641	L, H	1.0×10^{-3}
I_{sc}, A	5.16	I_{s1}, A	1.56×10^{-10}	C_{in}, F	70.0×10^{-6}
V_{oc}, V	21.6	I_{s2}, A	2.27×10^{-5}	C_{out}, F	330.0×10^{-6}
I_{mp}, A	4.63	R_s, Ω	0.1803	f, Hz	50.0×10^{3}
V_{mp}, V	17.3	R_{sh}, Ω	229.486	R_L, Ω	94.0
K_v, V/°C	-80×10^{-3}	a_1	0.9939		
K_i, A/°C	3.000×10^{-3}	a_2	2.006		
N_s	36.0				
N_p	1.0				

IET Renew. Power Gener., pp. 1–10

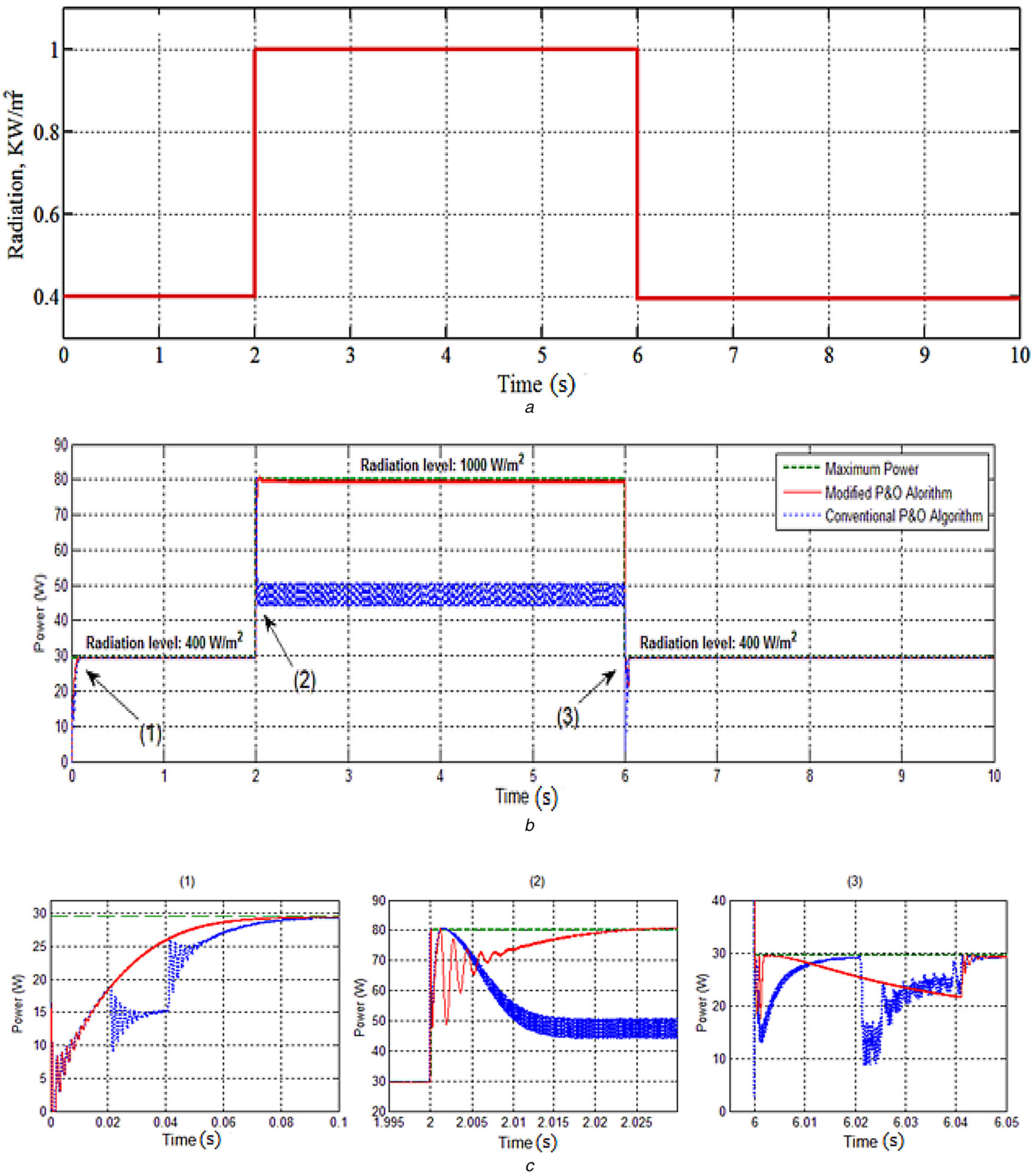

Fig. 6 *Simulation results for both algorithms*

a Conventional P&O and MP&O
b Change of radiation level
Selected zones form Fig. 6*a*(1), (2) and (3)

algorithm might miss new optimum points, which results in tracking failure of MPP [8, 10, 24] as shown in Fig. 6 ($t = 2$–6 s).

Fig. 6 also shows some selected times (1), (2) and (3) as subplots. They depict the dynamic response of both algorithms. Subplot (1) shows the dynamic response of both algorithms at start up. It shows results of both MPPT algorithms at initial solar radiation level of 0.4 KW/m^2 which corresponds to power variance from 0 to 29.5 W at time from 0 to 0.1 s. The figure shows a good time response of two algorithms but it is clear that the modified algorithm is faster than the conventional one. Subplots (2) and (3) show dynamic responses of both algorithms as a result of increasing and decreasing solar radiation. The dynamic response of modified algorithm is more clearly accurate. The conventional P&O algorithm oscillates and fails to track MPP at rapid increasing of solar radiation. Moreover, it has more undershoots than the modified one. The differences between both algorithms are not drastic in case of steady or gradual change of radiation. Table 2 shows the summary of steady-state simulation of conventional and MP&O algorithms. Table 2 shows the tracking factor of the PV system in percentage during weather variations. The tracking factor is the ratio between theoretical maximum power and maximum tracking power of the PV system, sometimes it is called tracking efficiency. The value of tracking factor for MP&O is larger than conventional P&O algorithm. On the other hand, power oscillation of MP&O is smaller than conventional P&O algorithm.

5 Implementation and experimental results

5.1 Methodology for experimentation and implementation

Fig. 7*a* shows the experimental environment used in the implementation and testing of the proposed modified algorithm. This figure not only shows the general MPPT operation but also clarifies the used methodology in experimentations. In the

Table 2 Average characteristics of steady-state simulation

<table>
<tr><th>Method</th><th colspan="2">Tracking factor</th><th colspan="2">Voltage ripple</th><th colspan="2">Power oscillation</th></tr>
<tr><td>time, s</td><td>3–4</td><td>7–8</td><td>3–4</td><td>7–8</td><td>3–4</td><td>7–8</td></tr>
<tr><td>P&O</td><td>56%</td><td>99%</td><td colspan="2">1.0%</td><td>15%</td><td>2.8%</td></tr>
<tr><td>MP&O</td><td>99%</td><td>99%</td><td colspan="2">1.0%</td><td>1.9%</td><td>1.9%</td></tr>
</table>

proposed methodology, solar energy level is continuously monitored using a solar power meter and the MPPT algorithm is executed within an embedded microcontroller system while data is logged and transferred to a computer.

Fig. 7*a* is presented in two main data paths. The first data path includes the PV module, the DC/DC converter, the MPPT system and the load. The second data path is where radiation and temperature measurements are collected directly from the sun. Solar radiation is measured and recorded during all experiments using a solar power meter from Lutron Electronics [36]. The temperature is also measured using a temperature measurement device. Solar and temperature data are not used during the normal operation of the MPPT. They are only used in the design phases prior implementation to ensure that the developed algorithm cope with the targeted environment variations. Therefore, the MP&O algorithm has no extra sensors needed. Only voltage and current need to be measured. On the other data path, solar radiation/temperature meters are continuously running during all experiments. They capture measurements each 5 s in a timed manner where each data measurement is associated with the real time/date. The results are stored within a memory card which is used to log the data to the PC.

Fig. 7*b* presents a diagram of the proposed methodology used to design and implement MPPT systems starting from an initial prototype to final system. The proposed methodology includes two main phases. Before the first phase starts, there is an initial prototype available in the lab. This prototype is a simple DC/DC converter circuit with an embedded development board for implementation of MPPT algorithms. The first phase includes a PC with MATLAB and the embedded development board running the modified MPPT algorithm. An HIL simulation model based on MATLAB/Simulink is used to verify the developed initial prototype running the proposed simulated modified algorithm. If the results from the HIL simulation have deviations from MPP, then modifications are applied to the initial prototype. Otherwise, another HIL simulation is applied using real measurements. In this step, real solar and temperature measurements are used instead of computer models, which forms a hybrid real/simulation environment. The second phase is an experimentation that is based on a real PV module and DC/DC converter. At this phase, the developed prototype is already tested with a hybrid real/simulation model. This increases its chances against real-world noise and uncertainties. However, the real-world experimentation may reveal further problems that require modifications to the initial prototype.

5.2 Implementation of the proposed MPPT algorithm

The Freescale FRDM-KL25Z development board is used for implementation of the proposed algorithm. It is a small, low-power and cost-effective evaluation and development system for quick application prototyping and demonstration [37]. It contains the ARM-Cortex M0+ processor which is equipped with many high

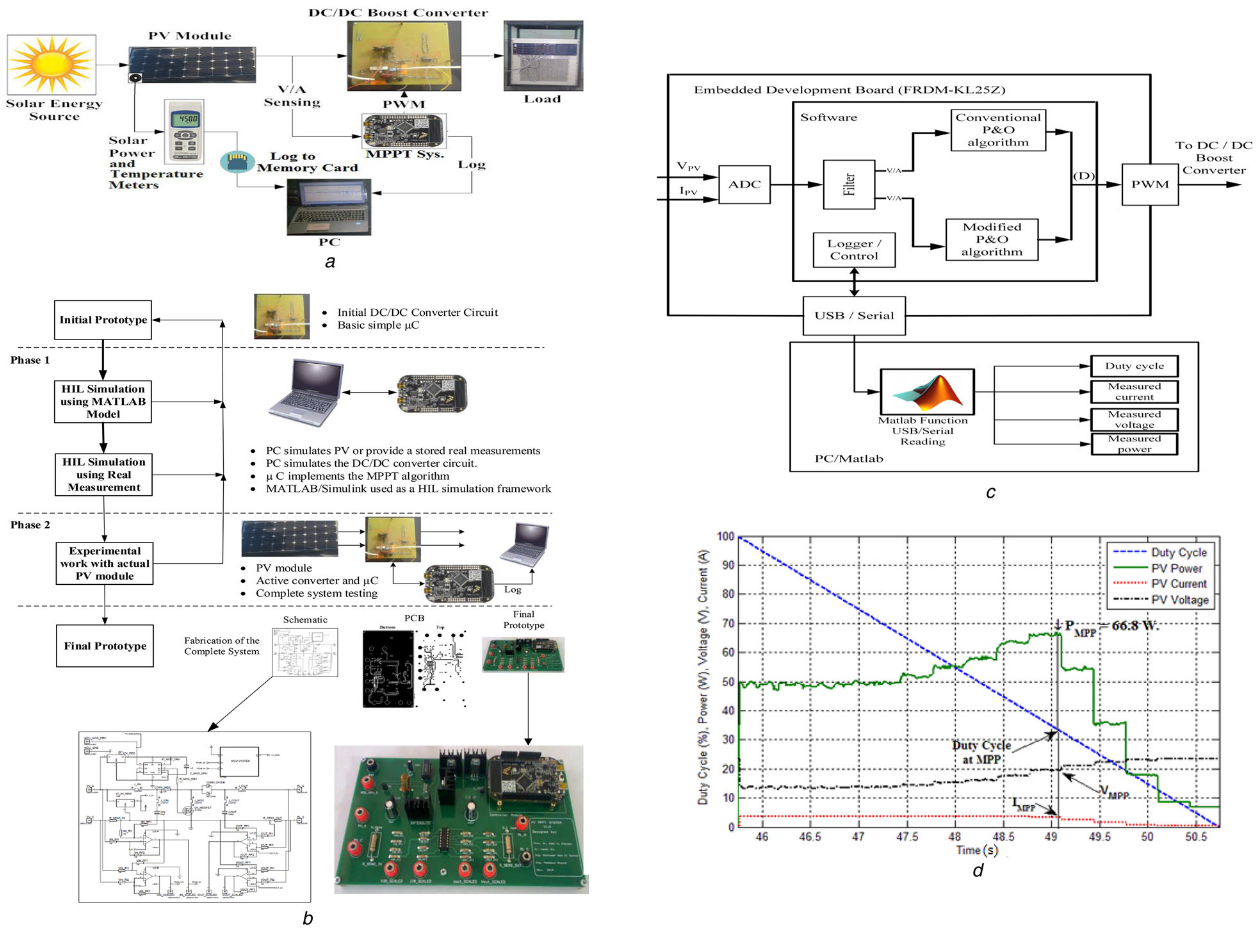

Fig. 7 *Experimental setup components*

a Setup of experimentation workstation
b HIL-based MPPT system testing and implementation methodology
c Embedded software for MPPT system
d MPP discovery experimental results

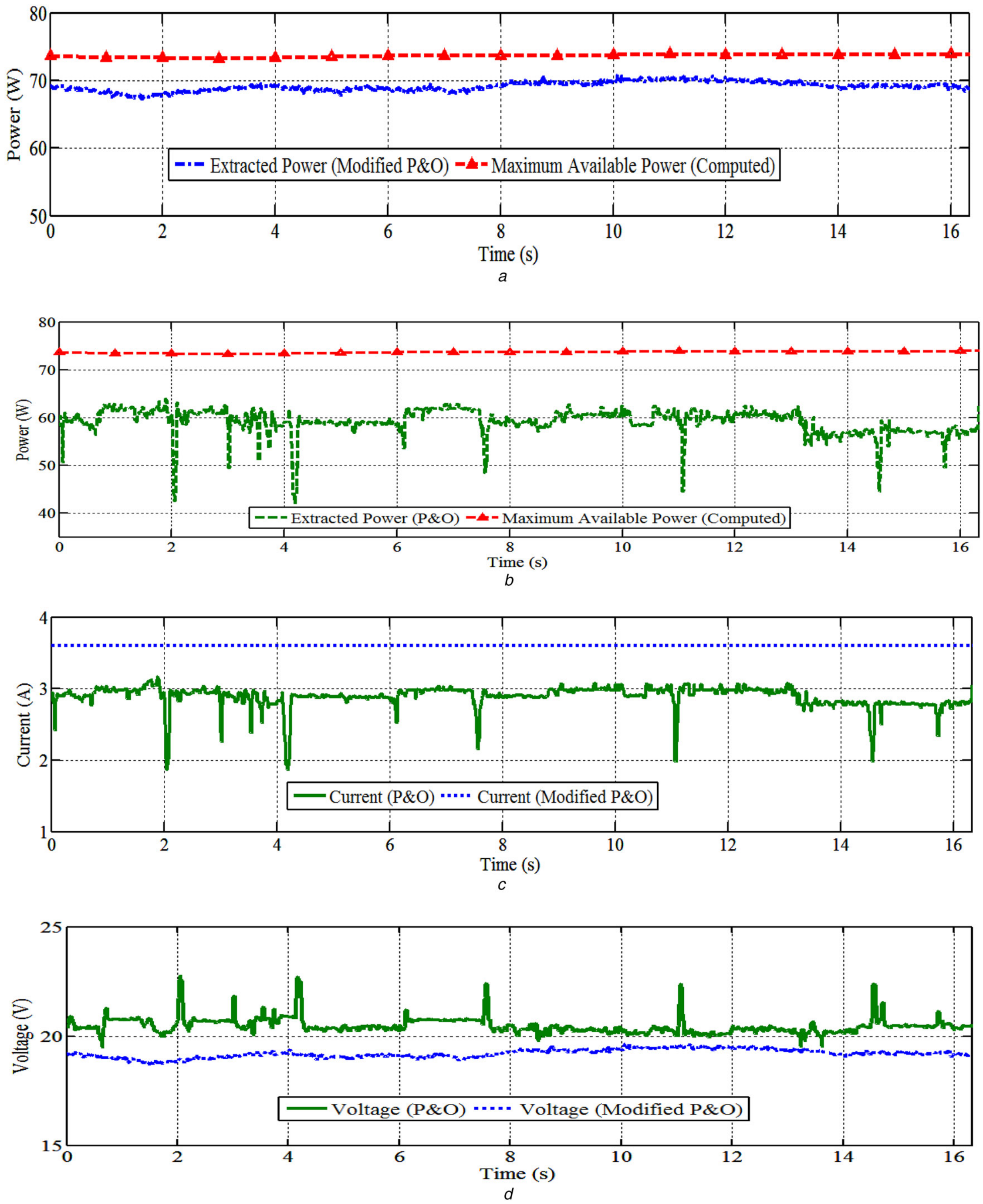

Fig. 8 *Steady-state experimental results for both algorithms*

a Modified algorithm during average radiation level: 950 W/m^2 at 01:00 PM
b Conventional algorithm during average radiation level: 855 W/m^2 at 01:30 PM
c PV module current values for both algorithms
d PV module voltage values for both algorithms

precision analogue-to-digital converters (ADC) and pulse-width modulation generation units making it very suitable for the MPPT systems. Fig. 7*c* shows the embedded software implemented within the FRDM-KL25Z development board. The conventional P&O algorithm and the MP&O algorithm are built into the development board.

The voltage (V_{pv}) and current (I_{pv}) are measured from the PV module and are fed to the FRDM-KL25Z development board's ADCs. The measured data are filtered using a software median filter. Then, one of two built-in algorithms is applied to find and track the MPP. Only one algorithm is active and running at a time. The selection of the active algorithm is based on a command from the PC.

5.3 MPP discovery

To investigate the performance and effectiveness of the proposed algorithm, the tracked power needs to be compared with the available maximum power from the PV module. Therefore, an algorithm that is capable of identifying the current maximum power value was developed. It is based on changing the PV module voltage and reveals the power according to each voltage value. This is achieved by scanning the value of the duty cycle of the DC/DC converter which in order changes the input voltage and input current. This is similar to drawing the power curve against voltage values. Fig. 7*d* shows an example of a MPP

Table 3 Average characteristics of steady-state operation (experimental)

Method	Tracking factor, %	Voltage ripple, %	Power oscillation, %
P&O	90	4.6	14.3
MP&O	96	1.5	5.1

discovery sessions. The required time for discovery is less than 5 s. It shows the discovery operation applied to the real PV module with the real DC/DC converter.

5.4 Experimental results

The presented system as deployed in our laboratory is currently used for further developments and experimentations. Fig. 8 shows the results logged from running the conventional and proposed algorithms at different steady state and implemented within the system. For each algorithm, the maximum power is calculated using the PV model and directly from the data logged using the solar radiation meter and temperature. It is also verified using the MPP discovery technique from the previous subsection. The figure reveals that the MP&O algorithm has less oscillation and more accuracy. It is also obvious that the MP&O algorithm is more robust. Table 3 shows the summary of steady-state experimental operation of both algorithms. From results of Fig. 8 and Table 3 it can be seen that the maximum power with its associated voltages and currents of the MP&O algorithm is more accurate, stable, reliable and less oscillating than conventional P&O algorithm.

6 Conclusion

This paper proposed a MP&O algorithm that is based on load technique to track MPP under rapid change of weather and minimise steady-state oscillation. The MP&O algorithm is simulated and verified experimentally using a 80 W PV module. MP&O is implemented using an embedded microcontroller-based real-time with combined of HIL and actual radiation/temperature measurements. Simulation results show the ability of MP&O algorithm to extract an accurate maximum power due to rapid changes of radiation with quick and high response. The extracting maximum power has minimum oscillations at steady state that is causing increase in the efficiency and accuracy of PV system performance. In addition, the high response of the MP&O algorithm within a short time to such variations result in the avoidance in energy loss compared with the conventional P&O algorithm. This energy loss occurs from conventional P&O algorithm due to fail tracking of maximum power and oscillation around MPP at steady state. Experimental results show that the MP&O algorithm is more stable, reliable and has less oscillating than conventional P&O algorithm.

7 References

1 Spagnuolo, G., Franquelo, L., Suntio, T., *et al.*: 'Grid-connected photovoltaic generation plants: components and operation', *IEEE Ind. Electron. Mag.*, 2013, **7**, (3), pp. 6–20

2 Kollimalla, K., Mishra, M.: 'Adaptive perturb & observe MPPT algorithm for photovoltaic system'. 2013 IEEE Power and Energy Conf. at Illinois (PECI), 2013, pp. 42–47

3 Omran, W.: 'Performance analysis of grid-connected photovoltaic systems'. PhD thesis, University of Waterloo, Waterloo, Ontario, Canada, 2010

4 Report to Congressional Requesters prepared by the United States General Accounting Office: 'Meeting future electricity demand will increase emissions of some harmful substances', October 2002. Available at http://www.gao.gov/new.items/d0349.pdf

5 Safari, A., Mekhilef, S.: 'Simulation and hardware implementation of incremental conductance MPPT with direct control method using cuk converter', *IEEE Trans. Ind. Electron.*, 2011, **58**, (4), pp. 1154–1161

6 Faranda, R., Leva, S.: 'Energy comparison of MPPT techniques for PV systems', *WSEAS Trans. Power Syst.*, 2008, **3**, (6), pp. 446–455

7 Nasr Allah, A., Saied, M., Mustafa, M., *et al.*: 'A survey of maximum PPT techniques of PV systems'. Browse Conf. Publications Energytech, 2012, pp. 1–17

8 Killi, M., Samanta, S.: 'Modified perturb and observe MPPT algorithm for drift avoidance in photovoltaic systems', *IEEE Trans. Ind. Electron.*, 2015, **PP**, (99), pp. 1–10

9 Joe-Air, J., Tsong-Liang, H., Ying-Tung, H., *et al.*: 'Maximum power tracking for photovoltaic power systems', *Tamkang J. Sci. Eng.*, 2005, **8**, pp. 147–153

10 Zegaoui, A., Aillerie, M., Petit, P., *et al.*: 'Comparison of two common maximum power point trackers by simulating of PV generators', *Energy Procedia*, 2011, **6**, pp. 678–687

11 Swathy, A., Archana, R.: 'Maximum power point tracking using modified incremental conductance for solar photovoltaic system', *Int. J. Eng. Innov. Technol. (IJEIT)*, 2013, **3**, (2), pp. 333–337

12 Solodovnik, E., Shengyi, L., Dougal, R.: 'Power controller design for maximum power tracking in solar installations', *IEEE Trans. Power Electron.*, 2004, **19**, pp. 1295–1304

13 Femia, N., Petrone, G., Spagnuolo, G., *et al.*: 'Optimization of perturb and observe maximum power point tracking method', *IEEE Trans. Power Electron.*, 2005, **20**, (4), pp. 963–973

14 Liu, F., Duan, S., Liu, B., *et al.*: 'A variable step size INC MPPT method for PV systems', *IEEE Trans. Ind. Electron.*, 2008, **55**, (7), pp. 2622–2628

15 Tey, K., Mekhilef, S.: 'Modified incremental conductance algorithm for photovoltaic system under partial shading conditions and load variation', *IEEE Trans. Ind. Electron.*, 2014, **61**, (10), pp. 5384–5392

16 Rawat, R., Chandel, S.: 'Hill climbing techniques for tracking maximum power point in solar photovoltaic systems-a review', *Int. J. Sustain. Dev. Green Econ. (IJSDGE)*, 2013, **2**, pp. 90–95

17 Esram, T., Chapman, P.: 'Comparison of photovoltaic array maximum power point tracking techniques', *IEEE Trans. Energy Convers.*, 2007, **22**, (2), pp. 439–449

18 Liu, F., Kang, Y., Duan, S., *et al.*: 'Comparison of P&O and hill climbing MPPT methods for grid-connected PV converter'. 3rd IEEE Conf. on Industrial Electronics and Applications, ICIEA 2008, 3–5 June 2008

19 Alajmi, B., Ahmed, K., Finney, S., *et al.*: 'Fuzzy logic- control approach of a modified hill-climbing method for maximum power point in micro grid standalone photovoltaic system', *IEEE Trans. Power Electron.*, 2011, **26**, (4), pp. 1022–1030

20 Messai, A., Mellit, A., Kalogirou, S., *et al.*: 'Maximum power point tracking using a GA optimized fuzzy logic controller and its FPGA implementation', *Sol. Energy*, 2011, **85**, pp. 265–277

21 Veerachary, M., Senjyu, T., Uezato, K.: 'Neural-network-based maximum-power-point tracking of coupled-inductor interleaved-boost-converter-supplied PV system using fuzzy controller', *IEEE Trans. Ind. Electron.*, 2003, **50**, (4), pp. 749–758

22 Bendib, B., Krim, F., Belmili, H., *et al.*: 'An intelligent MPPT approach based on neural-network voltage estimator and fuzzy controller, applied to a stand-alone PV system'. 2014 IEEE 23rd Int. Symp. on Industrial Electronics (ISIE), Istanbul, Turky, June 2014, pp. 404–409

23 Shaiek, Y., Smida, M., Sakly, A., *et al.*: 'Comparison between conventional methods and GA approach for maximum power point tracking of shaded solar PV generators', *Sol. Energy*, 2013, **90**, pp. 107–122

24 Ishaque, K., Salam, Z., Mekhilef, S., *et al.*: 'An improved particle swarm optimization (PSO)-based MPPT for PV with reducing steady-state oscillation', *IEEE Trans. Power Electron.*, 2012, **27**, (8), pp. 3627–3638

25 Renaudineau, H., Donatantonio, F., Fontchastagner, J., *et al.*: 'A PSO-based global MPPT technique for distributed PV power generation', *IEEE Trans. Ind. Electron.*, 2015, **62**, (2), pp. 1047–1058

26 Bianconi, E., Calvente, J., Giral, R., *et al.*: 'A fast current-based MPPT technique employing sliding mode control', *IEEE Trans. Ind. Electron.*, 2013, **60**, (3), pp. 1168–1178

27 Elbaset, A.A., Ali, H., Abd-El Sattar, M.: 'Novel seven-parameter model for photovoltaic modules', *Sol. Energy Mater. Sol. Cells*, 2014, **130**, pp. 442–455

28 Sharp Electronics Corporation: 'Poly-crystalline silicon photovoltaic module with 80 W maximum power [datasheet]' (Sharp Electronics Corporation, NY, USA, 2005)

29 Abouda, S., Frederic, N., Koubaa, Y., *et al.*: 'Design, simulation and voltage control of standalone photovoltaic system based MPPT: application to a pumping system', *Int. J. Renew. Energy Res.*, 2013, **3**, pp. 538–549

30 Hohm, D., Ropp, M.: 'Comparative study of maximum power point tracking algorithms', *Prog. Photovolt., Res. Appl.*, 2003, **11**, pp. 47–62

31 Tan, Y., Kirschen, D., Jenkins, N.: 'A model of PV generation suitable for stability analysis', *IEEE Trans. Energy Convers.*, 2004, **19**, (4), pp. 748–755

32 Sera, D., Kerekes, T., Teodorescu, R., *et al.*: 'Improved MPPT algorithms for rapidly changing environmental conditions'. 12th Int. Power Electronics and Motion Control Conf., 2006, pp. 1614–1619

33 Alqarni, M., Darwish, K.: 'Maximum power point tracking for photovoltaic system: modified perturb and observe algorithm'. 2012 47th IEEE Int. Universities Power Engineering Conf. (UPEC), 2012, pp. 1–4

34 Peftitsis, D., Adamidis, G., Balouktsis, A.: 'An investigation of new control method for MPPT in PV array using DC/DC buck–boost converter'. 2nd WSEAS/IASME Int. Conf. on Renewable Energy Sources (RES'08), Corfu, Greece, 2008, pp. 40–45

35 Rashid, M.: 'Power electronics hand book' (Academic press, New York, 2001)

36 Lutron Electronics: 'SOLAR POWER METER: SD card real time data recorder, patented spectral response: 400 to 1100 nm [datasheet]', 2012. Available at http://www.sunwe.com.tw/lutron/SPM-1116SD.pdf

37 http://www.keil.com/appnotes/files/apnt_232.pdf